Magnetic sensors

AlScN-Based SAW Magnetic Field Sensor for Isolated Closed-Loop Hysteretic Current Control of Switched-Mode Power Converters

Stefan Moench[1]*, Jana Marie Meyer[2], Agnė Žukauskaitė[1,3], Vadim Lebedev[1], Simon Fichtner[2,4]*, Jingxiang Su[2], Florian Niekiel[2], Thorsten Giese[2], Lars Thormählen[4], Eckhard Quandt[4], and Fabian Lofink[2]

[1]*Fraunhofer Institute for Applied Solid State Physics IAF, 79108 Freiburg, Germany*
[2]*Fraunhofer Institute for Silicon Technology ISIT, 25524 Itzehoe, Germany*
[3]*Fraunhofer Institute for Organic Electronics, Electron Beam and Plasma Technology FEP, 01277 Dresden, Germany*
[4]*Institute for Materials Science, Kiel University, 24143 Kiel, Germany*
**Member, IEEE*

Manuscript received 18 February 2022; revised 19 July 2022; accepted 8 September 2022. Date of publication 12 September 2022; date of current version 23 September 2022.

Abstract—This letter uses a surface acoustic wave magnetic field sensor for measurement and closed-loop current control of the inductor current in a GaN-based dc-dc power converter. The sensor is based on aluminium scandium nitride thin films with relatively high Sc concentration of 32% and fabricated on low-cost 8-in silicon substrate, with a magnetostrictive FeCoSiB film on top of a SAW delay line. The device has dc and bidirectional current measurement capability (derived from the magnetic flux density around a current trace) and is operated electrically isolated above the current trace. With permanent magnets as magnetic bias, the setup has a usable bidirectional current range of ±5 A. A phase detector IC measures the phase shift between the 296 MHz, 19 dBm input, and 35 dB attenuated output signal of the delay line sensor. The active sensor area has a distance of 2.5 mm from the current trace. In a 1.2 mT bias, the sensor is operated with a sensitivity of 18.28°/mT and bipolar current range of up to ±5 A. The sensor signal is enhanced by an analog filter to compensate the over 1 μs delay from the delay line and readout circuit. Finally, the sensor is used as the input of an analog hysteretic current control loop. The closed-loop current control operation is demonstrated using a 48 V GaN-based half-bridge dc-dc converter with 16 kHz triangular inductor current.

Index Terms—Magnetic sensors, sensor systems and applications, closed-loop systems, current sensors, surface acoustic waves, switching converters.

I. INTRODUCTION

Electrical current sensors are essential in a multitude of applications [1], [2], for example, control of power converters [3], power metering, motor drive, and overcurrent protection. Besides electrical requirements for current sensors such as bandwidth, dynamic range, and dc capability, also the size, cost, and the possibility for a non-invasive, electrically isolated measurement is decisive for the suitability in certain applications. One possible isolated sensing principle is to measure the magnetic flux density close to a current trace by a surface acoustic wave (SAW) sensor. There are two common design approaches either using a resonator or a delay line. Here, the delay line design was chosen as the interaction area between SAW and sensitive area is increased. The sensing principle utilizes the magnetoelastic effect of a magnetostrictive film (e.g., FeCoSiB) where the Young's modulus is changed by an external magnetic field (ΔE-effect), causing a change of the SAW phase velocity [4]. Exciting an interdigital transducer (IDT) on one port of the delay line with a high frequency sinusoidal signal and measuring the phase shift (signal delay) to the other port of the delay line gives a sensor signal sensitive to the magnetic field, caused by the current.

A promising material to fabricate such SAW sensors in thin-film technology is aluminium scandium nitride [5], [6] (AlScN), providing improved electromechanical coupling [7] compared to AlN [8], which is often used for SAW sensors. A more detailed description about electro-acoustic properties of AlScN determined with SAW resonators can be found in [7]. Furthermore, same as AlN, AlScN can be sputter-deposited on large diameter silicon substrates, enabling low sensor fabrication cost, compared to other single crystal materials used for SAW like quartz or $LiNbO_3$. Previously, an AlScN thin-film-based SAW magnetic field sensor with a magnetostrictive FeCoSiB layer between IDTs has been presented in [9] by the authors. Similar sensors based on other material systems and substrates have also been demonstrated [10], [11], [12], [13]. However, the application of such sensors in actual power converter control applications is rarely reported.

To fill this gap, this letter uses an AlScN thin film based SAW magnetic field sensor similar to [9] for closed-loop hysteretic current control of a switched-mode dc–dc power converter.

First, the SAW magnetic field sensor with high scandium concentration [14] is described and characterized (see Section II-A), using a phase detector as readout circuit (see Section II-B) under direct and current-induced magnetic fields (see Section II-C). Then, after discussion of the observed hysteresis (see Section II-D), the sensor signal is enhanced by a delay compensation filter (see Section II-E), and the zero current output is adjusted by variation of the excitation frequency (see Section II-F). Finally, the sensor is used as isolated, dc-capable, and bi-directional current sensor in a 48 V half-bridge

Corresponding author: Stefan Moench (e-mail: stefan.moench@iaf.fraunhofer.de)
Stefan Moench and Jana Marie Meyer contributed equally to this work.
Associate Editor: Matteo Rinaldi.
Digital Object Identifier 10.1109/LSENS.2022.3205853

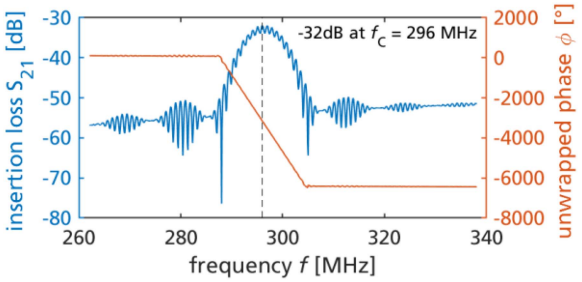

Fig. 1. Measured *S*-parameters around a center frequency of 296 MHz.

dc-dc power converter [15] for closed-loop hysteretic current control (see Section II-G).

II. EXPERIMENTS

A. Sensor Design and Characterization

A 1 μm $Al_{0.68}Sc_{0.32}N$ layer [14] is sputter deposited on a high-resistivity Si(001) wafer. 200 nm AlCu IDTs (periodicity of 16 μm), a delay line length $l = 3.8$ mm, and 25 finger pairs are the sensor interface. On top of a 1 μm thick guiding interlayer (SiO_2 smoothed with chemical mechanical polishing), a 200 nm magnetostrictive $(Fe_{90}Co_{10})_{78}Si_{12}B_{10}$ layer is deposited via RF magnetron sputtering [9].

Fig. 1 shows *S*-parameter measurements of the sensor. Around the SAW response center frequency of $f_C = 296$ MHz, the insertion loss is -32 dB and 22 dB higher than the -54 dB baseline. The unwrapped absolute phase shows a total change of -6360° for increasing frequencies, ±8.55 MHz around the center frequency. This virtual increase of 743.9°/MHz represents a delay time of $\Delta t = 1.03$ μs. From the delay line length l, the acoustic wave velocity $v = 3689$ m/s follows. The delay limits the sensor response time [16].

B. Readout Circuit

A 30 MHz phase detector IC (analog AD8302 [17]) on a board (AD8302-EVALZ) is used as readout circuit. A 19 dBm sinusoidal excitation signal is connected directly into the delay line and by a T-connector and 20 dB attenuator to one port of the phase detector (-1 dBm input level). The delay line output (-13 dBm) is connected to the other port of the phase detector. The nominal 10 mV/° gain and 30 MHz bandwidth of the phase detector is adjusted by an external gain-setting resistor R8 and filter capacitor C8 (see the datasheet [17]). The output signal (sensor signal) is measured (if not otherwise denoted) by an oscilloscope, which is later also used to measure the voltage and current waveforms of the controlled dc-dc converter.

Fig. 2 shows the setup, consisting of a dc–dc converter, the sensor, magnets, and a phase detector, further described in this letter.

C. Magnetic and Pulsed-Current Characterization

First, the sensor is characterized in a magnetic field, generated by two solenoids, using a lock-in amplifier to measure the phase change as in [9]. After magnetic saturation by ± 4.9 mT for 1 s, the flux density is swept between -2.5 and $+$ 2.5 mT in both directions. Fig. 3 shows the measured phase change with arrows indicating the

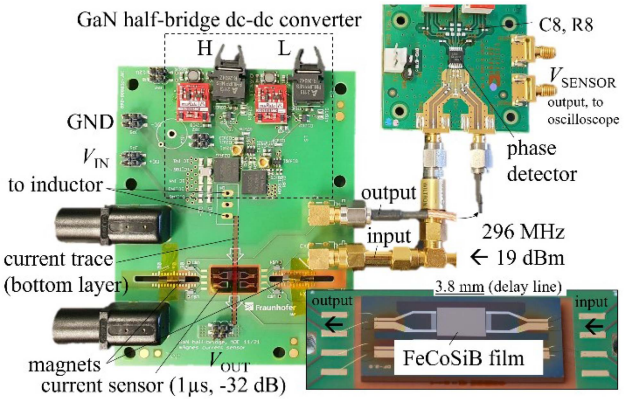

Fig. 2. Photo of the converter, sensor, magnets, and phase detector.

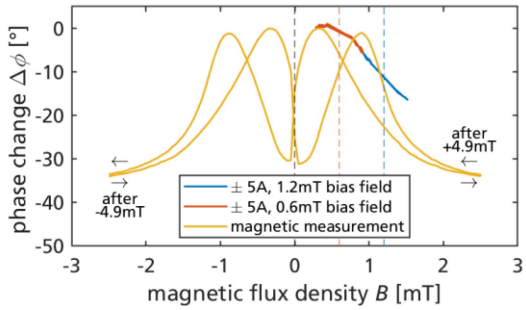

Fig. 3. Measured phase change depending on the magnetic flux density.

direction. A significant hysteresis is observed, especially around 0 mT.

The high sensitivity around 0 mT seems not suitable for sensor operation because of a limited high sensitivity range and due to the ambiguity in the course as the two branches of the hysteresis curve intersect at zero field. Further local maxima of sensitivity are 60° /mT (-1.1 mT), 34 /mT (-0.7 mT), 55°/mT (-0.35 mT), 60°/mT (0.3 mT), 32°/mT (0.6 mT), and 62°/mT (1.15 mT). To reduce the effect of the hysteresis, the range of magnetic flux density is reduced for the later sensor operation to below ±0.325 mT around the bias field that is sufficient for reversible operation for all above listed working points. N45 NdFeB permanent magnets placed on both sides of the sensor in the plane of the delay-line generate the bias field (see Fig. 2). For an offset of 0.6 mT, $2 \times 2 \times 4$ mm^3 magnets (separation of 36 mm) on both sides are used, and for 1.2 mT, $2 \times 2 \times 6$ mm^3 magnets (separation of 32 mm). From a 3-D EM-simulation of the sensor and current trace (2.5 mm below the sensor), the proportionality between the magnetic flux density and the current in the trace of 0.065 mT/A is extracted, which is a measurement range of ±5 A for the selected range of ±0.325 mT around a bias field. Next, the sensor is characterized with pulsed currents in a current trace below the sensor. 500 μs long current pulses were applied to the current trace, and the phase change acquired from the phase detector. Fig. 3 also shows the pulsed current results for 0.6/1.2 mT bias. At the higher offset of 1.2 mT a higher, monotonic, and more linear phase change is observed and thus used for further sensor application. The sensitivity within the ±5 A range is 1.188°/A, or 18.28°/mT, which is lower than the maximum observed sensitivity in the pure magnetic characterization. One reason for the lower sensitivity is that the actual bias field might differ from the intended one due to misalignment of the permanent magnets. The gain

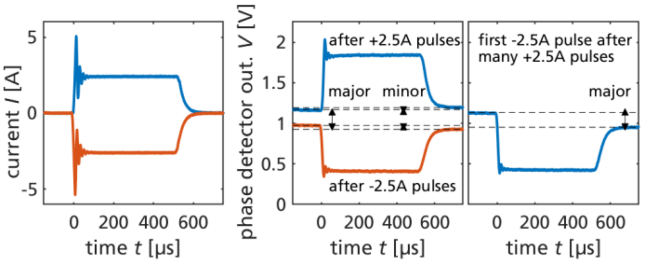

Fig. 4. Pulsed current (left) characterization shows hysteresis (right).

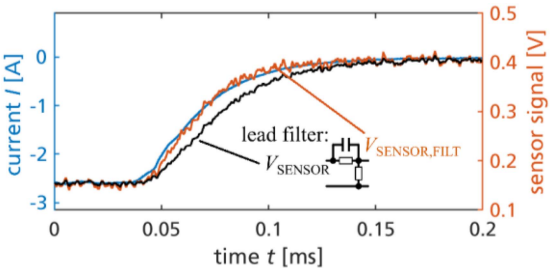

Fig. 5. Comparison of a current pulse (blue, 2.5 A) and the sensor signal after lead-compensation (orange), compared to the original sensor signal (black). The unfiltered signal is shown scaled by one-half.

from the phase detector is increased to 0.2 V/° using a gain setting resistor R8 = 380 kΩ; see [17], which also reduced the phase detector bandwidth to 1.5 MHz.

D. Magnetic Hysteresis in Bipolar Current Operation

The sensor is later used in a converter with bidirectional currents. The typical operation is with many similar positive current pulses followed by many similar negative current pulses, always returning to zero current (or a small current in the other direction). In this operation, the sensor operates in minor (low-hysteresis) magnetic loops over some time and not on major (high-hysteresis) magnetic loops. For example, the converter first operates mainly with a positive current waveform (between 0 A…+5 A) in charging/sourcing mode and later operates with a mainly negative current waveform (between 0 A…-5 A) in discharging/sinking mode. To investigate the severity of the hysteresis for this operation, more pulsed current measurements are carried out at further reduced peak currents of ±2.5 A.

Fig. 4 (left) shows the pulsed current signal (measured with a conventional current probe), where the current before and after the pulse is zero. Fig. 4 (middle) shows the sensor response after many consecutive positive or negative pulses. While the shift of the baseline within one measurement (minor loops, either many positive or negative pulses) is small and vanishes after many pulses, the difference between the positive and negative pulses is more significant [see Fig. 4 (right)]. Nevertheless, the sensor is still usable for control applications. Since the transition between positive and negative current operation in the converter is controlled by software, the major hysteresis might be compensated in software, similar to methods applied to other magnetic current sensors with hysteresis [18], [19]. The measurements in Fig. 4 use an additional filter capacitor ($C8 = 22$ pF, [17]) to reduce the signal noise, which reduced the effective bandwidth of the sensor here to 100 kHz. It is noted that the origin of the magnitude of hysteresis is not from the sign change of the bidirectional current (because a magnetic bias is used), but from the amplitude of the magnetic field change.

E. Delay Compensation

The bandwidth and delay (here 1 μs) of the current sensor limits the response time of a control loop. Furthermore, the increased gain setting of the phase detector and additional low-pass filter setting further reduces the bandwidth, which causes a total delay larger than the 1 μs from just the delay-line. In the later used analog current control, the sensor signal is compared to a reference signal to trigger switching actions. Since the current in a power converter is changing rapidly, the delay causes the switching actions to happen not immediately at the intended setpoints. This can cause too high currents and loss of controllability. As countermeasure, a lead-compensation filter can be used. A high-pass filtered signal of the sensor output is added to the sensor output by a passive filter. The current controlled in power converters is the inductor current, which is similar to a piecewise-linear waveform, for example, a triangular current. During increasing current transitions, an additional positive offset is added by the filter, and during decreasing current transitions, a negative offset is added to the sensor signal, both proportional to the rate of current change. This allows to reconstruct a filtered signal, which, after the time-constant of the filter (dimensioned to the total delay of the sensor and readout circuit), follows the actual non-delayed current signal. The filter is realized by the passive circuit shown in Fig. 5 (2 × 2.2 kΩ, 11 nF). The filtered signal $V_{\mathrm{SENSOR,FILT}}$ has halved the amplitude of the signal V_{SENSOR} from the phase detector.

Fig. 5 demonstrates the effectiveness of this approach for a 2.5 A transition. Here, the phase detector is configured for a gain of 0.2 V/° and bandwidth of 469 kHz ($C8 = 3.3$ pF [17]). The delay is clearly visible and is higher than 1 μs due to the bandwidth reduction. The enhanced signal also has a delay at the beginning of the pulse, but then quickly tracks the actual current waveform with little delay. The passive filter halves the amplitude the signal. This enhanced sensor signal enables a faster and more precise current control.

F. Adjustment of the Sensor Signal at Zero Current

The filtered sensor signal is now directly connected to the input of an analog hysteretic current controller (see [15]) implemented on a system-on-chip (Cypress PSoC 5LP). The controller expects a signal in the range 0…1 V, with 0.5 V representing 0 A. To center the output signal around 0.5 V, instead of an external offset amplifier circuit, in this letter the excitation frequency of the SAW was adjusted, which shifted the absolute value of the phase detector output. As shown in Fig. 1, the absolute phase change per excitation frequency change is 743.9°/MHz, and the sensor operates well not only at the center frequency of 296 MHz, but also slightly around this frequency. A frequency adjustment smaller than ±0.242 MHz is sufficient to cause ±180° absolute phase change. To adjust the signal level at zero current to 0.5 V, the frequency was thus slightly adjusted before the operation of the closed-loop control, in such way that the phase detector signal after the signal halving from the filter was centered around 0.5 V.

G. Closed-Loop Hysteretic Current Control

Fig. 6 shows a simplified schematic of the converter and hysteretic control. The converter is a GaN-based transistor half-bridge similar to [15]. The filtered sensed current signal is compared by fast analog voltage comparators to reference values (peak and valley current setpoints), which then trigger an set/reset (SR) flip-flop, which in turn changes the switch state of the half-bridge transistors. Both, the peak and valley, of the inductor current are controlled so that a variable switching frequency of the converter results. The reference

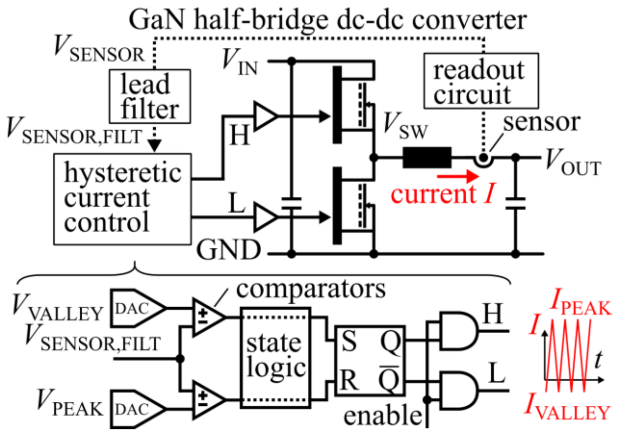

Fig. 6. Circuit of dc–dc converter, filter and hysteretic current control.

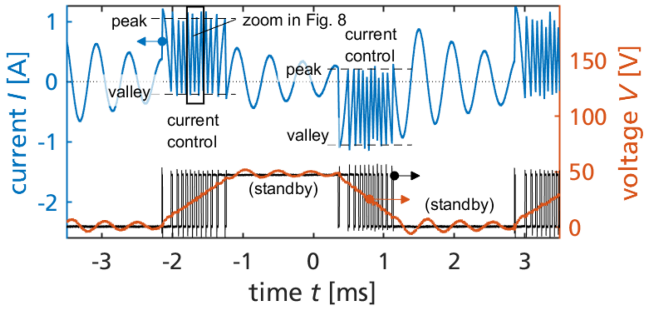

Fig. 7. Switching waveforms: Inductor current with peak/valley setpoints (dashed), switch-node and output (orange) voltage(black).

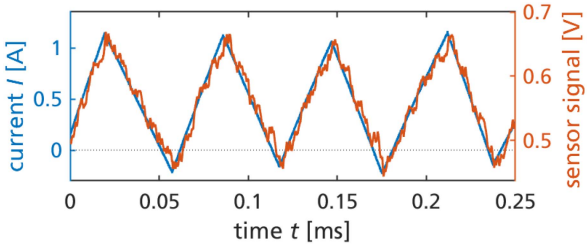

Fig. 8. Comparison of inductor current (measured with reference probe) and filtered signal from the SAW sensor.

values are generated by digital-to-analog converters and adjustable via software during operation. The converter is operated at 48 V input voltage, with a capacitive load connected to the output. With a cycle frequency of 200 Hz, the capacitor was charged and discharged between 0 and 48 V, by setting the peak/valley setpoints to around +1 A/-0.2 A during charging and +0.2 A/-1 A during discharging. Fig. 7 shows the resulting inductor current (blue) waveform with the setpoint values (dashed), and the switch-node voltage (black), as well as the output voltage (orange). Fig. 8 compares the inductor current measured by a conventional current probe with the filtered sensor signal. The switching waveform has up to 16 kHz switching frequency and is a zoom into the data from Fig. 7.

The results demonstrate that AlScN-based SAW magnetic field sensors are well suited for current sensing and control applications, such as power electronics. The sensor combines dc capability, an isolated measurement, the required bandwidth and sensitivity, with a low-cost fabrication on large diameter Si substrates.

ACKNOWLEDGMENT

This work was supported in part by the Fraunhofer Internal Programs under Grant MAVO 840 173 in the project »mAgnes«, and in part by the German Research Foundation (DFG) through the Collaborative Research Center CRC 1261.

REFERENCES

[1] S. Ziegler, R. C. Woodward, H. H. C. Iu, and L. J. Borle, "Current sensing techniques. A review," *IEEE Sensors J.*, vol. 9, no. 4, pp. 354–376, Apr. 2009. doi: 10.1109/JSEN.2009.2013914.

[2] P. Ripka, "Electric current sensors: A review," *Meas. Sci. Technol.*, vol. 21, no. 11, 2010, Art. no. 112001.

[3] F. Costa, P. Poulichet, F. Mazaleyrat, and E. Labouré, "The current sensors in power electronics, a review," *EPE J.*, vol. 11, no. 1, pp. 7–18, 2001.

[4] A. Kittmann et al., "Wide band low noise love wave magnetic field sensor system," *Sci. Rep.*, vol. 8, no. 1, p. 278, 2018.

[5] M. Akiyama, T. Kamohara, K. Kano, A. Teshigahara, Y. Takeuchi, and N. Kawahara, "Enhancement of piezoelectric response in scandium aluminum nitride alloy thin films prepared by dual reactive cosputtering," *Adv. Mater.*, vol. 21, no. 5, pp. 593–596, 2009.

[6] S. Fichtner et al., "AlScN: A III-V semiconductor based ferroelectric," *J. Appl. Phys.*, vol. 125, no. 11, 2019, Art. no. 114103.

[7] N. Kurz et al., "Experimental determination of the electro-acoustic properties of thin film AlScN using surface acoustic wave resonators," *J. Appl. Phys.*, vol. 126, no. 7, 2019, Art. no. 75106.

[8] G. Wingqvist, F. Tasnádi, A. Zukauskaite, J. Birch, H. Arwin, and L. Hultman, "Increased electromechanical coupling in w−ScxAl1−xN," *Appl. Phys. Lett.*, vol. 97 no. 11, 2010, Art. no. 112902.

[9] J. M. Meyer et al., "Thin-film-based SAW magnetic field sensors," *Sensors*, vol. 21, no. 24, 2021, Art. no. 8166.

[10] V. V. Kondalkar, X. Li, I. Park, S. S. Yang, and K. Lee, "Development of chipless, wireless current sensor system based on giant magnetoimpedance magnetic sensor and surface acoustic wave transponder," *Sci. Rep.*, vol. 8, no. 1, 2018, Art. no. 2401.

[11] F. Xu, W. Wang, X. Shao, X. Liu, and Y. Liang, "Optimization of surface acoustic wave-based rate sensors," *Sensors*, vol. 15, no. 10, pp. 25761–25773, 2015. doi: 10.3390/s151025761.

[12] V. Schell et al., "Magnetic anisotropy controlled FeCoSiB thin films for surface acoustic wave magnetic field sensors," *Appl. Phys. Lett.*, vol. 116, no. 7, 2020, Art. no. 73503.

[13] A. Kittmann et al., "Sensitivity and noise analysis of SAW magnetic field sensors with varied magnetostrictive layer thicknesses," *Sensors Actuators A, Phys.*, vol. 311, 2020, Art. no. 111998.

[14] Y. Lu et al., "Surface morphology and microstructure of pulsed DC magnetron sputtered piezoelectric AlN and AlScN thin films," *Phys. Status Solidi A*, vol. 215, no. 9, 2018, Art. no. 1700559.

[15] S. Moench et al., "A GaN-based DC-DC converter with zero voltage switching and hysteretic current control for 99% efficient bidirectional charging of electrocaloric capacitive loads," in *Proc. PCIM Eur. Int. Exhib. Conf. Power Electron., Intell. Motion, Renew. Energy Energy Manage.*, 2022, pp. 1–10.

[16] J. Labrenz et al., "Frequency response of SAW delay line magnetic field/current sensor," *IEEE Sensors Lett.*, vol. 3, no. 10, Oct. 2019, Art no. 1500404, doi: 10.1109/LSENS.2019.2943129.

[17] "Analog devices, AD8302 LF - 2.7 GHz RF/IF gain and phase detector datasheet," 2018. [Online]. Available: https://www.analog.com/media/en/technical-documentation/data-sheets/ad8302.pdf

[18] G. El Bacha, S. Milano, and J. Viola, "Allegro microsystems - Application Information 269114-AN: Hysteresis mitigation in current sensor ICs, 2015.

[19] J. Han, J. Hu, Y. Ouyang, S. X. Wang, and J. He, "Hysteretic modeling of output characteristics of giant magnetoresistive current sensors," *IEEE Trans. Ind. Electron.*, vol. 62, no. 1, pp. 516–524, Jan. 2015, doi: 10.1109/TIE.2014.2326989.